13. Coupled vibration of hoisting cable in cable-guided hoisting system with different swivels

Jinjie Wang[1], Guohua Cao[2], Mingxing Lin[3], Shanzeng Liu[4]
[1, 2, 4]School of Mechatronic Engineering, China University of Mining and Technology, Xuzhou, China
[1, 2]Jiangsu Key Laboratory of Mine Mechanical and Electrical, Xuzhou, China
[3]School of Mechanical Engineering, Shandong University, Jinan, China
[2]Corresponding author
E-mail: [1]*wangjinjie@cumt.edu.cn*, [2]*caoguohua@cumt.edu.cn*, [3]*mxlin@sdu.edu.cn*, [4]*liushanzeng@163.com*
(Received 2 October 2015; accepted 10 November 2015)

Abstract. In most cases, the hoisting cable in the cable-guided hoisting system is connected to the hoisting bucket with the swivel. The coupled longitudinal-torsional responses of the hoisting cable with time-varying length are investigated. The hoisting cable and two guiding cables are discretized by employing the assumed modes method, while the equations of motion are derived using Lagrange equations of the first kind, where a coefficient λ varying from 0 to 1 is introduced to represent the free spinning, proportional and self-locking swivels. The longitudinal and torsional displacements with different swivels are obtained. The results indicate the torsional displacement in the free spinning swivel is much larger than that in the proportional and there is one resonance in the former, while the longitudinal resonance in the free spinning swivel occurs earlier than that in the other two, which implies the system frequencies decrease. In addition, the presented model could also be used to describe the coupled vibration in the rigid rail-guided hoisting system but needs more modes.

Keywords: hoisting cable, coupled vibration, swivel, guiding cable.

1. Introduction

Cables, due to their light weight and their ability to resist relatively large axial loads, have been extensively employed in diverse engineering applications [1-3]. However, they are subjected to large-amplitude vibrations for their high flexibility and low internal damping. Thus, the dynamic behavior of cables has been studied widely for decades. Recently, the coupled vibration of the cable with time-varying length has attracted a great deal of attention and various approaches have been proposed. Wang et al. [4] analyzed the coupled lateral- transverse-longitudinal dynamics of an underwater, drawn cable with an attached mass. A variable-domain element is adopted to discretize the equations of motion. Later, Kaczmarczyk and Ostachowicz [5] exhibited the coupled lateral-longitudinal dynamic response of the catenary-vertical ropes in the deep mine hoisting system and obtained the numerical solution by using the Rayleigh-Ritz method. Zhang et al. [6] presented the coupled lateral-longitudinal vibration model of the vertically translating elevator cables subjected to the general initial conditions and the external excitation with Galerkin method. Ren and Zhu [7] presented the longitudinal and lateral vibrations of a moving two-cable one-rigid-body-car system, in which the rotation of the car is considered.

Cables are characterized by the coupled longitudinal-torsional behavior when subjected to the external loads. Therefore, the vibration analysis of the coupled axial-torsional cable is of great significance. Samras [8] tested experimentally the coupling coefficients and discovered that the axial-torsional stiffness coefficient is approximately equal to the torsional-axial stiffness coefficient. Hashemi and Roach [9] presented the derivation of a dynamic finite element for the coupled extension-torsion vibration analysis of the cable and evaluated the coupled frequencies.

However, few researchers concentrated on the coupled longitudinal -torsional dynamic responses of the hoisting cable with time-varying length, caused by the external displacement excitation. Some problems have arisen in the hoisting cable of cable-guided hoisting system shown in Fig. 1, which is used to sink the deep vertical shaft [10]. This system is mainly composed of one hoisting cable, two guiding cables, a hoisting bucket and a swivel, where the semi rotation

resistant cable (18×7) is connected to the bucket with the swivel. The most commonly used swivel is the free spinning swivel. During loading and unloading, the free spinning swivel will always rotate back and forth, causing a series of effects: the tension-torsion stresses caused by the rotation will considerably reduce the wire rope's fatigue strength, especially in the vicinity of the swivel [11]. However, the self-locking swivel, a more sophisticated version, is designed to prevent the cables from unlaying. On the one hand, the torsion of hoisting cable is easy to destroy the electric cables wound around the surface of the hoisting cable; on the other hand, the torsion of cable aggravates the longitudinal vibration of itself and brings about the slight rotation of the bucket. These two facts reduce the performance of rescue capsules greatly both on safety and comfort. Therefore, it is significant to recognize the essential difference between two kinds of swivels.

This paper is organized as follows. In Section 2, the coupled vibration model is established by adopting Lagrangian multipliers. Particularly, a coefficientλvarying from 0 to 1 is introduced to represent the free spinning, proportional and self-locking swivels. In Section 3, the results of the longitudinal and torsional responses from different swivels are analyzed and compared. Finally, Section 4 draws some conclusions.

2. Theoretical investigation

For simplicity, the hoisting system can be modelled as one vertically translating model described by a cylindrical coordinate system. This model is composed of one hoisting cable of length $l(t)$ at time instant t, two guiding cables of length L and one bucket with mass m attached to the lower end of the hoisting cable. The bucket is supported by the two guiding cables through two guide sleeves. The upper ends of two guiding cables are fixed to the derrick and the lower ends are constrained laterally and tensioned by the preloads T_{b1} and T_{b2}; the displacements $u(x,t)$, $\theta(x,t)u_1$ and θ_1 represent the longitudinal and torsional vibrations of the hoisting cable and the bucket, respectively; y_1 and y_2 depict the lateral vibrations of the guiding cables; a and b denote the distances from the hoisting cable to the left and right guiding cables. The harmonic excitation $e(t)$ at position $x = 0$ caused by the out-of-round head sheave should be considered because of resonance.

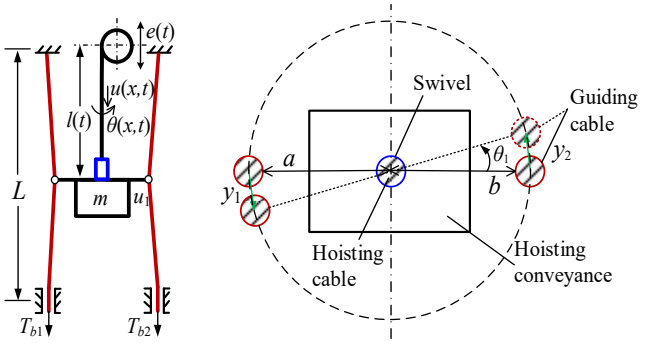

Fig. 1. Schematic diagrams of cable-guided hoisting system, front and top views

2.1. Spatial discretization

The kinetic energy T of hoisting cable can be expressed as:

$$T = \frac{1}{2}\int_0^{l(t)}\left[\rho_1\left(\frac{Du}{Dt}+v\right)^2 + J_1\left(\frac{D\theta}{Dt}\right)^2\right]dx + \frac{1}{2}\int_0^{L}\sum_{i=1}^{2}\rho_2\left(\frac{\partial y_i}{\partial t}\right)^2 dx + \frac{J}{2}\left(\frac{d\theta_1}{dt}\right)^2 + \frac{m}{2}\left(\frac{du_1}{dt}+v\right)^2, \quad (1)$$

where ρ_1 and ρ_2 are the mass per unit length the hoisting cable and the guiding cable; J_1 and J are the moment of inertia of the hoisting cable the bucket, respectively.

The total potential energy V of the system can be represented as:

$$V = \int_0^{l(t)} \left\{ \frac{1}{2} \left[\left(Q_1 \frac{\partial u}{\partial x} + Q_2 \frac{\partial \theta}{\partial x} \right) \frac{\partial u}{\partial x} + \left(Q_3 \frac{\partial u}{\partial x} + Q_4 \frac{\partial \theta}{\partial x} \right) \frac{\partial \theta}{\partial x} \right] + T_0 \frac{\partial u}{\partial x} \right\} dx + \int_0^L \sum_{i=1}^{2} \frac{T_i(x)}{2} \left(\frac{\partial y_i}{\partial x} \right)^2 dx - \int_0^{l(t)} \rho_1 g u dx - mg(u_1 + l), \tag{2}$$

where Q_1, Q_2, Q_3 and Q_4 are the axial, axial-torsional coupling, torsional-axial coupling, and torsional stiffness coefficients of the hoisting cable, respectively. The approximation $Q_{23} = Q_2 = Q_3$ will be adopted in the following derivation [7]. The tensions in the hoisting cable and the guiding cables are expressed:

$$T_0(x,t) = [m + \rho_1(l(t) - x)]g, \quad T_i(x) = T_{bi} + \rho_2 g(L - x). \tag{3}$$

The geometric boundary conditions for the hoisting cable and the guiding cables are obtained as:

$$u(0,t) = 0, \quad \theta(0,t) = 0, \quad y_i(0,t) = 0, \quad y_i(L,t) = 0, \quad (i = 1,2). \tag{4}$$

The geometric matching conditions at the interface between the hoisting cable and the conveyance are:

$$u_1 = u(l,t), \quad \theta_1 = \lambda\theta(l,t), \quad (0 \le \lambda \le 1), \tag{5}$$

where $\lambda = 0$ and 1 denote the free spinning and self-locking swivels, while $0 < \lambda < 1$ denotes the proportional swivel.

The conditions between the conveyance and the guiding cables are:

$$2a\sin\frac{\theta_1}{2} - y_1(l,t) = 0, \quad 2b\sin\frac{\theta_1}{2} + y_2(l,t) = 0. \tag{6}$$

For simplicity, herein two new dimensionless parameters $\xi = x/l(t)$ and $\eta = x/L$ are introduced and the time-varying domain $[0, l(t)]$ and the time-invariant $[0, L]$ for x are both transformed to a time-invariant $[0,1]$ for ξ and η. Hence, the dependent variable $u(x,t)$, $\theta(x,t)$ and $y_i(x,t)$ become $\hat{u}(\xi,t)$, $\hat{\theta}(\xi,t)$ and $\hat{y}_i(\eta,t)$, respectively. Further, the partial derivatives of $u(x,t)$ with respect to x and t are related to those of $\hat{u}(\xi,t)$ with respect to ξ and t:

$$u_x = \frac{1}{l(t)}\hat{u}_\xi, \quad u_t = \hat{u}_t - \frac{v\xi}{l(t)}\hat{u}_\xi, \quad \theta_x = \frac{1}{l(t)}\hat{\theta}_\xi, \quad \theta_t = \hat{\theta}_t - \frac{v\xi}{l(t)}\hat{\theta}_\xi,$$
$$y_{i,x} = \frac{1}{L}\hat{y}_{i,\eta}, \quad y_{i,t} = \hat{y}_{i,t}. \tag{7}$$

The similar derivations are presented as:

$$T_0(x,t) = \hat{T}_0(\xi,t) = [m + \rho_1 l(t)(1-\xi)]g, \quad T_i(x) = \hat{T}_i(\eta) = T_{bi} + \rho_2 gL(1-\eta). \tag{8}$$

Accordingly, the boundary conditions in Eq. (4) become:

$$\hat{u}(0,t) = 0, \quad \hat{\theta}(0,t) = 0, \quad \hat{y}_i(0,t) = 0, \quad \hat{y}_i(1,t) = 0, \quad (i = 1,2). \tag{9}$$

Considering the torsional displacement of the hoisting bucket is slight, the linear approximation $\sin\theta \approx \theta$ is adopted and Eq. (6) becomes:

$$\hat{u}(1,t) - u_1 = 0, \;\; \lambda\hat{\theta}(1,t) - \theta_1 = 0, \;\; \hat{y}_1\left(\frac{l}{L},t\right) - a\theta_1 = 0, \;\; \hat{y}_2\left(\frac{l}{L},t\right) + b\theta_1 = 0. \tag{10}$$

The displacements can be approximated by expansions of a complete set of trial functions and expressed as:

$$\begin{aligned} u(\xi,t) &= \sum_{i=1}^{n} U_{1,i}(\xi)q_{1,i}(t), \;\; \theta(\xi,t) = \sum_{i=1}^{n} U_{2,i}(\xi)q_{2,i}(t), \\ \hat{y}_1(\eta,t) &= \sum_{i=1}^{n} W_{1,i}(\eta)q_{3,i}(t), \;\; \hat{y}_2(\eta,t) = \sum_{i=1}^{n} W_{2,i}(\eta)q_{4,i}(t), \end{aligned} \tag{11}$$

where n represents the number of included modes; $q_{j,i}(t)$ are the generalized coordinates; $U_{j,i}$ and $W_{j,i}$ are the trial functions and should satisfy the homogeneous boundary conditions in Eq. (9), which can be expressed as:

$$U_{1,i}(\xi) = U_{2,i}(\xi) = \sqrt{2}\sin\left(\frac{2i-1}{2}\pi\xi\right), \;\; W_{1,i}(\eta) = W_{2,i}(\eta) = \sqrt{2}\sin(i\pi\eta). \tag{12}$$

Substituting Eqs. (1)-(2) into Lagrange equations of the first kind [12]:

$$\frac{d}{dt}\frac{\partial T}{\partial \dot{q}_i} - \frac{\partial T}{\partial q_i} + \frac{\partial V}{\partial q_i} = \sum_{j=1}^{2} \lambda_j \frac{\partial g_j}{\partial q_i}, \tag{13}$$

yields the equations of motion:

$$\mathbf{M}\ddot{\mathbf{q}} + \mathbf{C}\dot{\mathbf{q}} + \mathbf{K}\mathbf{q} = \mathbf{F} + \mathbf{G}^T\lambda, \;\; \mathbf{g}(\mathbf{q},t) = 0, \tag{14}$$

where $\mathbf{q} = (q_{1,1}, q_{2,1}, q_{3,1}, q_{4,1}, q_{1,2}, q_{2,2}, q_{3,2}, q_{4,2}, \cdots, q_{1,n}, q_{2,n}, q_{3,n}, q_{4,n}, q_{4n+1}, q_{4n+2})^T$ is the vector of generalized coordinates and it should be noted that these $(4n+2)$ generalized coordinates are not independent, however, the geometric matching conditions Eq. (10) yield the holonomic constraints $\mathbf{g}$ of the generalized coordinates, where $\mathbf{g} = (g_1, g_2)^T$ is a vector including all the constraint conditions in Eq. (10); $\mathbf{G} = \partial\mathbf{g}/\partial\mathbf{q}$ is the Jacobian of the constraint equations, which is a $4 \times (4n+2)$ matrix; and $\lambda = (\lambda_1, \lambda_2, \lambda_3, \lambda_4)^T$, which are called the Lagrangian multipliers. The matrices **M**, **C**, **K** and **F** are expressed as:

$$\mathbf{M}_{ij} = \begin{cases} \int_0^1 \rho_1 l U_{1,i}(\xi)U_{1,j}(\xi)d\xi, & (i,j \le n), \\ \int_0^1 J_1 l U_{2,i-n}(\xi)U_{2,j-n}(\xi)d\xi, & (n < i,j \le 2n), \\ \int_0^1 \rho_2 L W_{1,i-2n}(\eta)W_{1,j-2n}(\eta)d\eta, & (2n < i,j \le 3n), \\ \int_0^1 \rho_2 L W_{2,i-3n}(\eta)W_{2,j-3n}(\eta)d\eta, & (3n < i,j \le 4n), \\ m, & (i,j = 4n+1), \\ J, & (i,j = 4n+2), \end{cases}$$

$$\mathbf{C}_{ij}=\begin{cases}\left(\begin{array}{l}\rho_1 v\int_0^1(1-\xi)\left[U'_{1,i}(\xi)U_{1,j}(\xi)-U_{1,i}(\xi)U'_{1,j}(\xi)\right]d\xi\\ +\rho_1 v\int_0^1 U_{1,i}(\xi)U_{1,j}(\xi)d\xi,\quad (i,j\le n)\end{array}\right),\\ 0,\quad (n<i,j\le 4n+2),\end{cases}$$

$$\mathbf{K}_{ij}=\begin{cases}\left(\begin{array}{l}\frac{Q_1}{l}\int_0^1 U'_{1,i}(\xi)U'_{1,j}(\xi)d\xi+\rho_1 a\int_0^1(1-\xi)U'_{1,i}(\xi)U_{1,j}(\xi)d\xi\\ +\frac{\rho_1 v^2}{l}\int_0^1[\xi U'_{1,i}(\xi)U_{1,j}(\xi)-(1-\xi)^2U'_{1,i}(\xi)U'_{1,j}(\xi)]d\xi,\quad (i,j\le n)\end{array}\right),\\ \frac{Q_{23}}{l}\int_0^1 U'_{1,i-n}(\xi)U'_{2,j}(\xi)d\xi,\quad (n<i\le 2n,j\le n),\\ \frac{Q_4}{l}\int_0^1 U'_{2,i-n}(\xi)U'_{2,j-n}(\xi)d\xi,\quad (n<i,j\le 2n),\\ \frac{Q_{23}}{l}\int_0^1 U'_{2,i}(\xi)U'_{1,j-n}(\xi)d\xi,\quad (i\le n,n<j\le 2n),\\ \frac{1}{L}\int_0^1\hat{T}_1(\eta)W'_{1,i-2n}(\eta)W'_{1,j-2n}(\eta)d\eta,\quad (2n<i,j\le 3n),\\ \frac{1}{L}\int_0^1\hat{T}_2(\eta)W'_{2,i-3n}(\eta)W'_{2,j-3n}(\eta)d\eta,\quad (3n<i,j\le 4n),\\ 0,\quad (4n<i,j\le 4n+2).\end{cases}$$

$$\mathbf{F}_i=\begin{cases}\left(\begin{array}{l}\rho_1 v^2\int_0^1[(1-\xi)U'_{0,i}(\xi)-U_{0,i}(\xi)]d\xi+\rho_1 l\int_0^1(g-a)U_{0,i}(\xi)d\xi\\ -\int_0^1[mg+\rho_1 gl(1-\xi)]U'_{0,i}(\xi)d\xi,\quad (i\le n)\end{array}\right),\\ 0,\quad (n<i\le 4n),\\ m(g-a),\quad (i=4n+1),\\ 0,\quad (i=4n+2).\end{cases}$$

2.2. DAEs to ODEs for solution

Considering the constraint conditions in Eq. (10) are both linear algebraic equations, Eq. (14), a system of DAEs, could be transformed to ODEs. Thus, the second equation in Eq. (14) could be expressed in the form [13]:

$$\mathbf{g}(\mathbf{q},t)=\mathbf{G}(t)\mathbf{q}+\mathbf{g}_r(t)=\mathbf{0}, \tag{15}$$

where $\mathbf{g}_r(t)=\mathbf{0}$. Without loss of generality, suppose:

$$\mathbf{G}(t)=(\mathbf{G}_0\quad \mathbf{G}_1),\ \ \mathbf{q}=[\mathbf{q}_0^T\ \ \mathbf{q}_1^T]^T, \tag{16}$$

where $\mathbf{G}_0$ must be a nonsingular 4×4 matric, because its inverse matrix will be used subsequently. By Eqs. (10)-(12), one can obtain:

$$\mathbf{G}(t)=\begin{bmatrix} U_{1,1}(1),0,0,0 & U_{1,2}(1),0,0,0 & \cdots & U_{1,n}(1),0,0,0 & -1 & 0 \\ 0,\lambda U_{2,1}(1),0,0 & 0,\lambda U_{2,2}(1),0,0 & \cdots & 0,\lambda U_{2,n}(1),0,0 & 0 & -1 \\ 0,0,W_{1,1}\left(\frac{l}{L}\right),0 & 0,0,W_{1,2}\left(\frac{l}{L}\right),0 & \cdots & 0,0,W_{1,n}\left(\frac{l}{L}\right),0 & 0 & -a \\ 0,0,0,W_{2,1}\left(\frac{l}{L}\right) & 0,0,0,W_{2,2}\left(\frac{l}{L}\right) & \cdots & 0,0,0,W_{2,n}\left(\frac{l}{L}\right) & 0 & b \end{bmatrix},$$

$$\mathbf{G}_0=\begin{bmatrix} U_{1,1}(1) & 0 & 0 & 0 \\ 0 & \lambda U_{2,1}(1) & 0 & 0 \\ 0 & 0 & W_{1,1}\left(\frac{l}{L}\right) & 0 \\ 0 & 0 & 0 & W_{2,1}\left(\frac{l}{L}\right) \end{bmatrix},$$

$$\mathbf{G}_1=\begin{bmatrix} U_{1,2}(1),0,0,0 & \cdots & U_{1,n}(1),0,0,0 & -1 & 0 \\ 0,\lambda U_{2,2}(1),0,0 & \cdots & 0,\lambda U_{2,n}(1),0,0 & 0 & -1 \\ 0,0,W_{1,2}\left(\frac{l}{L}\right),0 & \cdots & 0,0,W_{1,n}\left(\frac{l}{L}\right),0 & 0 & -a \\ 0,0,0,W_{2,2}\left(\frac{l}{L}\right) & \cdots & 0,0,0,W_{2,n}\left(\frac{l}{L}\right) & 0 & b \end{bmatrix},$$

$\mathbf{q}_0=[q_{1,1},q_{2,1},q_{3,1},q_{4,1}]^T$,

$\mathbf{q}_1=[q_{1,2},q_{2,2},q_{3,2},q_{4,2},\cdots,q_{1,n},q_{2,n},q_{3,n},q_{4,n},q_{4n+1},q_{4n+2}]^T$.

By Substituting Eq. (16) into Eq. (15), one has:

$$\mathbf{q}=\Phi(t)\mathbf{q}_1,\ \ \Phi(t)=\begin{bmatrix}-\mathbf{G}_0^{-1}\mathbf{G}_1\\ \mathbf{I}\end{bmatrix}, \tag{17}$$

where $\mathbf{q}_1$, a $(4n-2)$ vector, become the new generalized coordinates, which are linearly independent; $\mathbf{I}$ is a $(4n-2)$ identity matrix.

Differentiating Eq. (17) twice yields:

$$\dot{\mathbf{q}}=\Phi(t)\dot{\mathbf{q}}_1+\dot{\Phi}(t)\mathbf{q}_1,\ \ \ddot{\mathbf{q}}=\Phi(t)\ddot{\mathbf{q}}_1+2\dot{\Phi}(t)\dot{\mathbf{q}}_1+\ddot{\Phi}(t)\mathbf{q}_1. \tag{18}$$

Eq. (16) multiplied by Eq. (17) can yield $\mathbf{G}\Phi=\mathbf{0}$. Substituting Eq. (18) into the first equation in Eq. (14), premultiplying by Φ^T and using the relations $\Phi^T\mathbf{G}^T=(\mathbf{G}\Phi)^T=\mathbf{0}$ yield:

$$\mathbf{M}_G\ddot{\mathbf{q}}_1+\mathbf{C}_G\dot{\mathbf{q}}_1+\mathbf{K}_G\mathbf{q}_1=\mathbf{F}_G, \tag{19}$$

with:

$$\mathbf{M}_G=\Phi^T\mathbf{M}\Phi,\ \ \mathbf{C}_G=2\Phi^T\mathbf{M}\dot{\Phi}+\Phi^T\mathbf{C}\Phi,\ \ \mathbf{K}_G=\Phi^T\mathbf{M}\ddot{\Phi}+\Phi^T\mathbf{C}\dot{\Phi}+\Phi^T\mathbf{K}\Phi,\ \ \mathbf{F}_G=\Phi^T\mathbf{F}. \tag{20}$$

Eq. (19) can be solved by an ODE solver. $\mathbf{q}$ can be assembled as:

$$\mathbf{q}=\begin{bmatrix}-\mathbf{G}_0^{-1}\mathbf{G}_1\mathbf{q}_1\\ \mathbf{q}_1\end{bmatrix}. \tag{21}$$

3. Results and discussion

Consider a hoisting cable with $\rho_1=0.4$ kg/m, $J_1=2\times10^{-5}$ kg·m, $Q_1=3.46\times10^7$ N, $Q_{23}=1.2\times10^5$ N·m and $Q_4=660$ N·m^2. The mass m and the moment of inertia J of the bucket are 2000 kg and 50 kg·m. The total length L of the hoisting cable is 244 m and the initial length

$l(0)$ is 4 m. The length of the guiding cable with $\rho_2 = 0.2$ kg/m is 250 m. The preloads T_{b1} and T_{b2} are both 1.5×10^4 N. The vertical excitation applied to the head sheave is $e(t) = 0.003\sin(4\pi t)$ m. The maximum velocity and acceleration are 6 m/s and 2 m/s^2, respectively. The total simulation time is 50 s and the time step size is 0.01 s. The number of included modes is $n = 10$, unless otherwise stated.

The torsional displacements of the lower end of the hoisting cable $\theta(l,t)$ and the bucket θ_1 are calculated when $\lambda = 0.5$ and shown in Fig. 2. The rotation of the bucket inevitably causes the lateral vibration of the guiding cables. The whole displacements of two guiding cables y_1 and y_2 at $t = 22$ and 32 s are shown in Fig. 3.

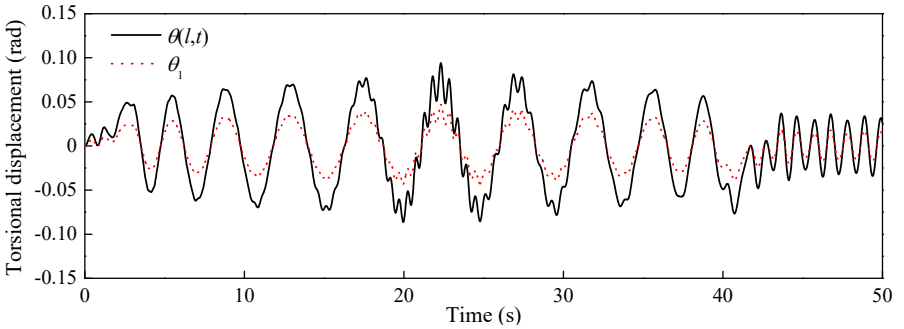

Fig. 2. Torsional displacements $\theta(l,t)$ and θ_1 with $\lambda = 0.5$

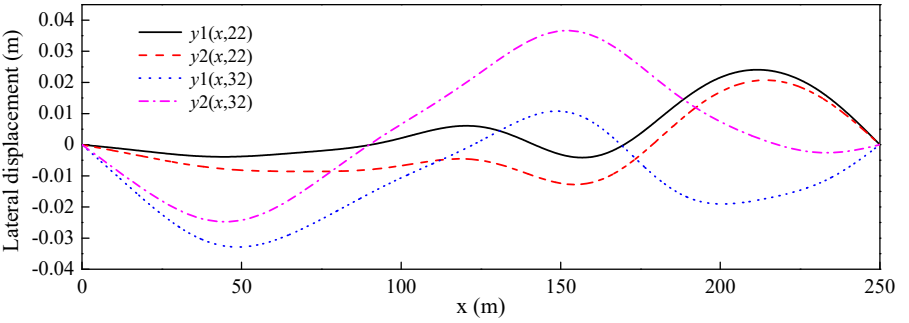

Fig. 3. Lateral displacements y_1 and y_2 at different times with $\lambda = 0.5$

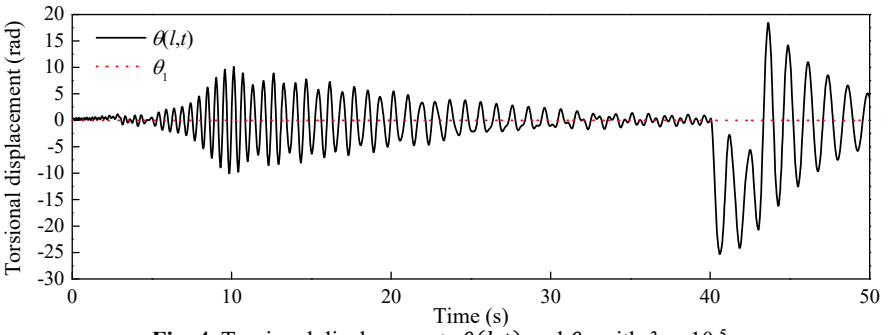

Fig. 4. Torsional displacements $\theta(l,t)$ and θ_1 with $\lambda = 10^{-5}$

In order to simulate the free spinning swivel, λ should be zero, however, this will result in the singular matrix $\mathbf{G}_0$ in Eq. (16). Thus, a fairly small number $\lambda = 10^{-5}$ is adopted. The torsional displacements of the lower end of the hoisting cable $\theta(l,t)$ and the bucket θ_1 are shown in Fig. 4. It can be observed that the torsional displacement of the bucket is almost zero. So are the lateral displacements of two guiding cables y_1 and y_2, and almost keep pace with each other, which is

shown in Fig. 5. By comparing Fig. 4 with Fig. 2, on the one hand, the torsional displacement in the free spinning swivel is much larger than that in the proportional swivel, on the other hand, there is one resonance at 10 s in Fig. 4.

The longitudinal displacements u_1 with three kinds of swivels are compared and shown in Fig. 6. Fig. 6 indicates there is no difference in longitudinal vibration u_1 between the self-locking swivel and the proportional one, and there is one resonance at 23 s. However, the longitudinal displacement with the free spinning swivel is obviously different and the resonance occurs at 10 s, which implies the system frequencies decrease.

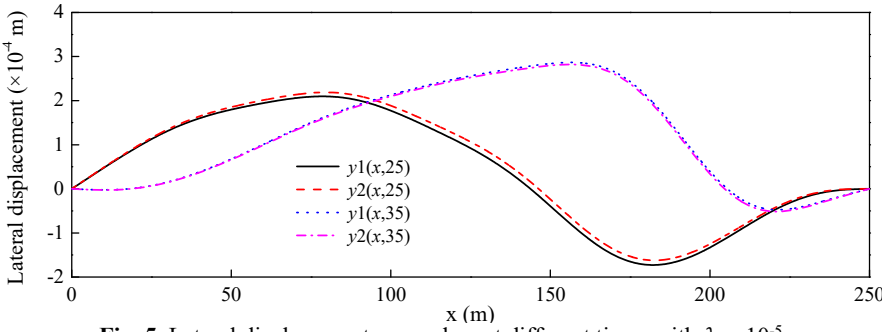

Fig. 5. Lateral displacements y_1 and y_2 at different times with $\lambda = 10^{-5}$

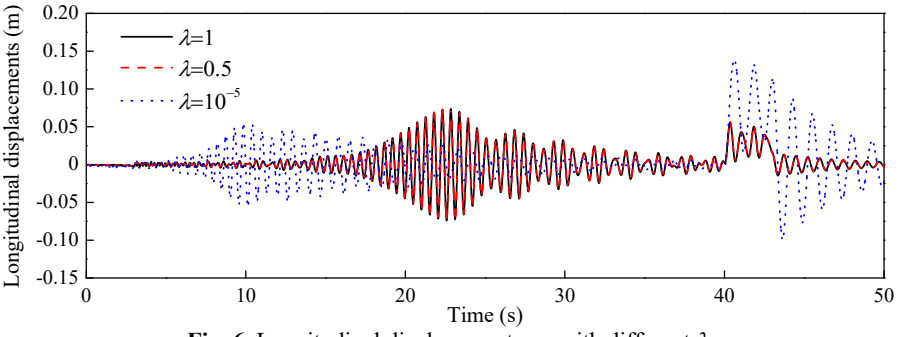

Fig. 6. Longitudinal displacements u_1 with different λ

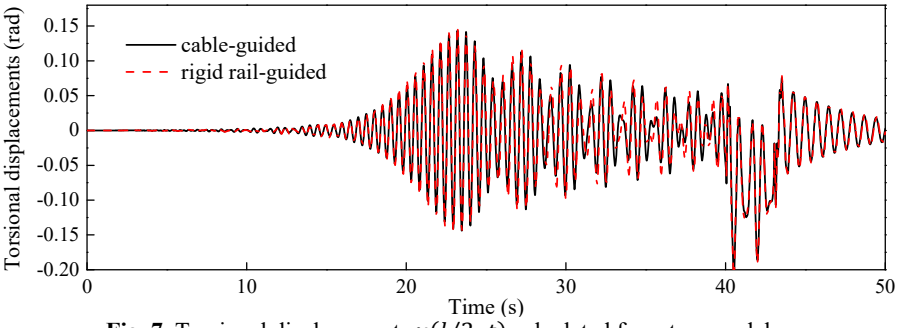

Fig. 7. Torsional displacements $u(l/2, t)$ calculated from two models

The presented theoretical model is derived from the cable-guided hoisting system, however, it would be excited if the model could be also applied to the rigid rail-guided hoisting system, such as the elevator system. The preloads T_{b1} and T_{b2} are increased to 10^8 N so that the guiding cables look like the rigid guide rail. The torsional displacement of the middle of the hoisting cable calculated using the presented model with $n = 30$ is compared with that from the rigid rail-guided model in Fig. 7. Although the trial functions in Eq. (12) in two models are different, the excellent

agreement indicates the presented model is generic and universal.

4. Conclusions

The coupled longitudinal-torsional responses of the hoisting cable with time-varying length in the cable-guided hoisting system are investigated. The vibration model is established by introducing a coefficient λ, which represents the free spinning, proportional and self-locking swivels when varying from 0 to 1. Especially, $\lambda = 10^{-5}$ or 10^{-6} is recommended for the free spinning swivel, otherwise, $\mathbf{G}_0$ will be a singular matrix. The presented theoretical model could also be used to describe the coupled vibration in the rigid rail-guided hoisting system but needs more modes.

Acknowledgements

This work is supported by the National Natural Science Foundation of China (51475456), Program for New Century Excellent Talents in University (NCET-13-1017) and the Priority Academic Program Development of Jiangsu Higher Education Institutions (PAPD).

References

[1] **Ma C., Xiao X. M.** Kinetic analysis of a multi-rope friction mine hoist under overload conditions. Journal of Vibroengineering, Vol. 15, Issue 2, 2013, p. 925-932.

[2] **Zi B., Qian S., Ding H. F., Andres K.** Design and analysis of cooperative cable parallel manipulators for multiple mobile cranes. International Journal of Advanced Robotic Systems, Vol. 9, 2012, p. 1-10.

[3] **Zhu W. D., Ren H.** A linear model of stationary elevator traveling and compensation cables. Journal of Sound and Vibration, Vol. 332, Issue 12, 2013, p. 3086-3097.

[4] **Wang P. H., Fung R. F., Lee M. J.** Finite element analysis of a three-dimensional underwater cable with time-dependent length. Journal of Sound and Vibration, Vol. 209, Issue 2, 1998, p. 223-249.

[5] **Kaczmarczyk S., Ostachowicz W.** Transient vibration phenomena in deep mine hoisting cables. Part 1: Mathematical model. Journal of Sound and Vibration, Vol. 262, Issue 2, 2003, p. 219-244.

[6] **Zhang P., Zhu C. M., Zhang L. J.** Analysis of forced coupled longitudinal-transverse vibration of flexible hoisting system with varying length. Engineering Mechanics, Vol. 25, Issue 12, 2008, p. 202-207.

[7] **Ren H., Zhu W. D.** An accurate spatial discretization and substructure method with application to moving elevator cable-car systems. Part 2: Application. Journal of Vibration and Acoustics, Transactions of the ASME, Vol. 135, Issue 5, 2013, p. 051037.

[8] **Samras R. K., Skop R. A., Milburn D. A.** Analysis of coupled extensional torsional oscillations in wire rope. Journal of Engineering for Industry, Vol. 96, 1974, p. 1130-1135.

[9] **Hashemi S. M., Roach A.** A dynamic finite element for vibration analysis of cables and wire ropes. Asian Journal of Civil Engineering, Vol. 7, Issue 5, 2006, p. 487-500.

[10] **Shao X. G., Zhu Z. C., Wang Q. G., Chen P. C., Zi B., Cao G. H.** Non-smooth dynamical analysis and experimental validation of the cable-suspended parallel manipulator. Proceedings of the Institution of Mechanical Engineers, Part C: Journal of Mechanical Engineering Science, Vol. 226, Issue 10, 2012, p. 2456-2466.

[11] **Verreet R., Ridge I. M. L.** The use of swivels with steel wire ropes. OIPEEC Round Table Conference, Bethlehem, USA, 2001.

[12] **Lanczos C.** The Variational Principles of Mechanics. Dover Publications, New York, 1986.

[13] **Ilchmann A., Reis T.** Surveys in Differential-Algebraic Equations 2. Springer-Verlag, Berlin, Germany, 2015.